Omnidirectional elastic band gap in finite lamellar structures

D. Bria[1,2] and B. Djafari-Rouhani[2]

[1]*Laboratoire de Dynamique et d'Optique des Matériaux, Département de Physique. Faculté des Sciences, Université Mohamed I, Boîte Postale 524, 60000 Oujda, Morocco*

[2]*Laboratoire de Dynamique et Structure des Matériaux Moléculaires, UPRESA CNRS 8024, UFR de Physique, Université de Lille 1, 59655 Villeneuve d'Ascq, France*

(Received 26 July 2002; published 21 November 2002)

This paper presents a comprehensive theoretical analysis of the occurrence of omnidirectional reflection in one-dimensional phononic crystal structures. We discuss the conditions for a one-dimensional layered structure, made of elastic materials, to exhibit total reflection of acoustic incident waves in a given frequency range, for all incident angles and all polarizations. The property of omnidirectional reflection can be fulfilled with a simple finite superlattice if the substrate from which the incident waves are launched is made of a material with high acoustic velocities (this is very similar to the case of omnidirectional optical mirror where the incident light is generated in vacuum). However, if the substrate is made of a material with low acoustic velocities, we propose two solutions to obtain an omnidirectional band gap, namely, the cladding of a superlattice with a layer of high acoustic velocities, which acts like a barrier for the propagation of phonons, or the association in tandem of two different superlattices in such a way that the superposition of their band structures exhibits an absolute acoustic band gap. We discuss the appropriate choices of the material and geometrical properties to realize such structures. The behavior of the transmission coefficients are discussed in relation with the dispersion curves of the finite structure embedded between two substrates. Both transmission coefficients and densities of states (from which we derive the dispersion curves) are calculated in the framework of a Green's function method.

DOI: 10.1103/PhysRevE.66.056609 PACS number(s): 42.70.Qs, 68.35.Gy, 68.35.Ja, 68.65.−k

I. INTRODUCTION

During the last few years, much attention has been devoted to the study of two- and three-dimensional (2D and 3D) periodic phononic crystals [1–7]. In analogy to the more familiar photonic crystals [8], the essential property of these structures is the existence of forbidden frequency bands, where the propagation of sound and ultrasonic vibrations is inhibited in any direction of space. Such phononic band gap materials can have practical applications such as acoustic filters [9], ultrasonic silent blocks [10], acoustic mirrors, and improvements in the design of piezoelectric ultrasonic transducers [11]. The contrast in elastic properties and densities between the constituents of the composite system is a critical parameter in determining the existence and the width of absolute band gaps.

In the field of photonic band gap materials, it has been argued during the last few years [12–14] that one-dimensional structures such as superlattices can also exhibit the property of omnidirectional reflection, i.e., the existence of a band gap for any incident wave independent of the incidence angle and polarization. However, because the photonic band structure of a superlattice does not display any absolute band gap (i.e., a gap for any value of the wave vector), the property of omnidirectional reflection holds in general when the incident light is launched from vacuum, or from a medium with relatively low index of refraction (or high velocity of light). To overcome this difficulty, when the incident light is generated in a high refraction index medium, we have recently proposed [15] to associate with the superlattice a cladding layer with a low index of refraction, which acts like a barrier for the propagation of light.

The object of this paper is to examine the possibility of realizing one-dimensional structures that exhibit the property of omnidirectional reflection for acoustic waves. In the frequency range of the omnidirectional reflection, the structure will behave analogously to the case of 2D and 3D phononic crystals, i.e., it reflects any acoustic wave independent of its polarization and incidence angle. We shall show that a simple superlattice can fulfill this property, provided the substrate from which the incident waves are launched is made of a material with relatively high acoustic velocities of sound. However, the substrate may have relatively low acoustic velocities, according to the large varieties in the elastic properties of materials. Then, we propose two alternative solutions to overcome the difficulty related to the choice of the substrate, in order to obtain a frequency domain in which the transmission of sound waves is inhibited even for a substrate with low velocities of sound. As mentioned in the case of photonic band gap materials, one solution would be to associate the superlattice with a cladding layer having high velocities of sound in order to create a barrier for the propagation of acoustic waves. Another solution will consist of associating two superlattices chosen appropriately in such a way that the superposition of their band structures displays a complete acoustic band gap. These ideas have been proposed very recently in two short communications [16,17]. In this paper, we present a comprehensive investigation of the conditions necessary for obtaining this acoustic gap and its evolution according to the physical parameters defining the one-dimensional structure. More precisely, the transmission spectra for different polarizations of the incident waves are calculated and analyzed in relation with the dispersion curves of the modes associated with the finite structure em-

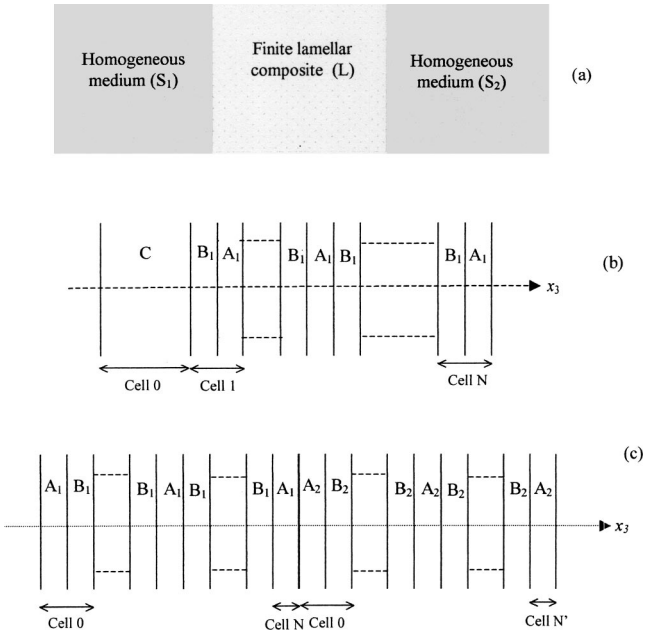

FIG. 1. Geometries of the omnidirectional band gap structure. (a) A finite lamellar composite system L embedded between two homogenous media S_1 and S_2. (b) The system L is constituted by a superlattice cladded with a material C. (c) The system L is constituted by a combination in tandem of two different superlattices.

bedded between the two substrates. When a maximum threshold for transmittance is imposed, we investigate the contributions of the different modes induced by the finite structure (bulk phonons of the superlattices, modes of the caldding layer, and interface modes) to the transmission spectra, thus revealing the limitations on the existence of an absolute band gap. We discuss the dependence of the transmission coefficients upon the thickness of the clad layer and the number of cells in the superlattices, as well as upon the choice of the layers in the superlattice, which are in contact with the substrates and with the clad. Specific illustrations are given for a finite Al/W superlattice cladded by a Si layer, and a combination in tandem of finite Al/W and Fe/epoxy superlattices. The transmission coefficients as well as the density of states, from which one can derive the dispersion curves, are calculated in the framework of a Green's function method.

A brief presentation of the model and method of calculation is presented in Sec. II. Section III contains the numerical illustrations as well as the discussion of the transmission coefficients for the occurrence of an omnidirectional band gap. Conclusions are given in Sec. IV.

II. MODEL AND METHOD OF CALCULATION

The geometries studied in this paper are schematically depicted in Fig. 1. We consider a finite lamellar structure **L** sandwiched between two substrates S_1 and S_2 [Fig. 1(a)]. The details about the composition of the finite structure are sketched in Figs. 1(b) and 1(c). In one case [Fig. 1(b)], the lamellar structure is composed of a finite superlattice containing alternating layers of materials A and B, and a clad layer of material C. Let us notice that in our calculation, the material C can be embedded inside the superlattice instead of being at its boundary. In the second geometry [Fig. 1(c)], two finite superlattices made, respectively, of materials (A_1, B_1) and (A_2, B_2) are associated together in tandem.

All the interfaces are taken to be parallel to (x_1, x_2) plane of a Cartesian coordinates system. All the media are assumed to be isotropic elastic media characterized by their mass densities, their transverse velocity C_t, and longitudinal velocity C_l of sound. Due to the isotropy within the (x_1, x_2) plane, the transverse elastic (or shear horizontal) waves, polarized perpendicular to the sagittal plane (x_1, x_3), are decoupled from sagittal waves polarized within this plane, for any value of the propagation vector $k_{\|}$ (parallel to the interfaces).

The study of acoustic wave propagation in such a composite lamellar system is performed by using a Green's function formalism based on the method of interface response theory [18]. In this theory, we calculate the Green's function of a composite system containing a large number of interfaces that separate different homogenous media. The density of states, the dispersion curves as well as the transmittance through finite substructures are obtained from the knowledge of the corresponding Green's function **g** that can be written in the composite material [19] as

$$g(DD)=G(DD)+G(DM)\{[G(MM)]^{-1}g(MM)\times[G(MM)]^{-1}-[G(MM)]^{-1}\}G(MD). \quad (1)$$

D and M denote, respectively, the whole space and the interface space in the composite material. G is a block diagonal matrix in which each sub-block G_i corresponds to the bulk Green's function of the subsystem i. One can notice that all the matrix elements $g(DD)$ of the final Green's function can be obtained once we know the matrix elements $g(MM)$ of g in the interface space M. The latter are obtained [13] by writing the matrix $g^{-1}(MM)$ as a sum of the submatrices $g_i^{-1}(MM)$ in each sub-block i considered separately. All details about the semianalytical calculation of the Green's function for infinite or semi-infinite superlattices as well as for a finite superlattice in contact with a substrate can be found in Ref. [20].

The transmission coefficients through the lamellar structure depicted in Fig. 1(a) can be calculated in the following way. An incident propagating vector $U(D)$ of the reference system depicted by the above $G(DD)$ generates in the composite system the following vector [19] $u(D)$ representing all the scattered (reflected and transmitted) waves:

$$u(D)=U(D)+G(DM)\{[G(MM)]^{-1}g(MM)[G(MM)]^{-1}-[G(MM)]^{-1}\}U(M). \quad (2)$$

On the other hand, one can also calculate the density of states of the final system. More precisely, the difference in the density of states (DOS) between the present composite system and a reference system formed out of three independent parts (the substrates S_1 and S_2 and the finite composite medium **L**) is given by [21]

$$\Delta n(\omega) = -\frac{1}{\pi}\frac{d}{d\omega}\arg \mathrm{Det}\left[\frac{g_L(MM)[g_{S_1}(00)g_{S_2}(00)]^{1/2}}{g(MM)}\right]. \tag{3}$$

Here $g_{S_1}(MM)$, $g_{S_2}(MM)$, and $g_L(MM)$ are, respectively, the Green's functions associated with the separated semi-infinite substrates S_1 and S_2, and the finite composite medium **L**.

The dispersion curves are obtained from the peaks in the density of states which are associated with the modes of the medium **L** interacting with the continuum of substrate modes. We shall focus our attention on transmitted waves through the lamellar composite system, in relation with the dispersion curves. The existence of an omnidirectional acoustic gap requires that the transmission coefficients fall below a threshold value for all polarizations and any incidence angle of the incoming waves. Let us notice that the incident wave, generated in the substrate S_1, can have three different polarizations; namely, transverse horizontal (or shear horizontal), transverse vertical, and longitudinal.

III. NUMERICAL RESULTS AND DISCUSSIONS

In this section, we show that omnidirectional reflection of acoustic waves can be achieved with only 1D systems instead of 2D or 3D phononic crystals. First, we emphasize that a single superlattice can display an omnidirectional reflection band, provided the substrate is made of a material with relatively high velocities of sound. Then, in order to remove the limitation about the choice of the substrate, we consider the geometries described in Fig. 1 where either a clad layer is added to the superlattice, or two different superlattices with appropriately chosen parameters are combined in tandem.

Let us first examine the so-called projected band structure of a superlattice, i.e., the frequency ω versus the wave vector $k_\parallel$. Figure 2 displays the phononic band structure of an infinite superlattice composed of Al and W materials with thicknesses d_1 and d_2, such as $d_1 = d_2 = 0.5D$, D being the period of the superlattice. We have used a dimensionless frequency $\Omega = \omega D/C_t(\mathrm{Al})$, where $C_t(\mathrm{Al})$ is the transverse velocity of sound in Al (the elastic parameters of the materials are listed in Table I). The left and right panels, respectively, give the band structure for transverse and sagittal acoustic waves. For every value of $k_\parallel$, the shaded and white areas in the projected band structure, respectively, correspond to the minibands and to the minigaps of the superlattice, where the propagation of acoustic waves is allowed or forbidden. Due to the large contrast between the elastic parameters of Al and W, the minigaps of the superlattice are rather large in contrast to the case of other systems such as GaAs-AlAs superlattices. Nevertheless, it can be easily noticed that the band structure shown in Fig. 2 does not display any absolute gap, this means a gap existing for every value of the wave vector $k_\parallel$. However, the superlattice can display an omnidirectional reflection band in the frequency range of the minigap ($2.952 < \Omega < 4.585$) if the velocities of sound in the substrate are high enough. More precisely, let us assume that the transverse velocity of sound in the substrate $C_t(s)$ is greater than 5543 m/s, (the heavy line in Fig. 2 indicates the sound line with the velocity 5543 m/s). For any wave launched from this substrate, the frequency will be situated above the sound line $\omega = C_t(s)k_\parallel$, i.e., above the heavy line in Fig. 2. When the frequency falls in the range $2.952 < \Omega < 4.585$ (corresponding to the minigap of the superlattice at $k_\parallel = 0$), the wave cannot propagate inside the superlattice and will be reflected back. Thus, the frequency range $2.952 < \Omega < 4.585$ corresponds to an omnidirectional reflection band for the chosen substrate. Generally speaking, the above condition expresses that the cone defined by the transverse velocity of sound in the substrate contains a minigap of the superlattice. With the Al/W superlattice, this condition is, for instance, fulfilled if the substrate is made of Si [11]. Of course, in practice, due to the finiteness of the omnidirectional mirror, one can only impose that the transmittance remains below a given threshold (for instance, 10^{-3} or 10^{-2}).

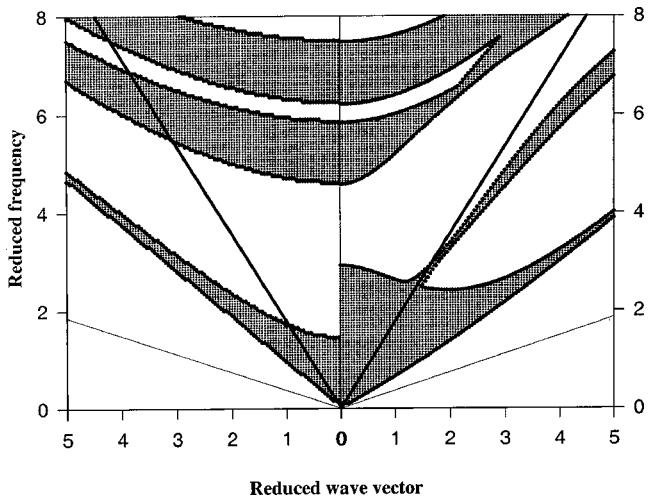

FIG. 2. Projected band structure of sagittal (right panel) and transverse (left panel) elastic waves in a W/AL superlattice. The reduced frequency $\Omega = \omega D/C_t(\mathrm{Al})$ is presented as a function of the reduced wave vector $k_\parallel D$. The shaded and white areas, respectively, correspond to the minibands and minigaps of the superlattice. The heavy and thin straight lines correspond, respectively, to sound velocities equal to 5543 and 1160 m/s (epoxy).

On the contrary, if the incident wave is initiated in a substrate made of a material with low velocities of sound such as epoxy [with $Ct(s) = 1160$ m/s, see the thin straight line in Fig. 2], the wave is not prohibited from propagation inside

TABLE I. Elastic parameters of the materials involved in the calculations.

Materials	Mass density (in kg m^{-3})	C_l (in m s^{-1})	C_t (in m s^{-1})
Al	2700	6422	3110
W	19300	5231	2860
Si	2330	8440	5845
Fe	8133	4757	2669
Epoxy	1200	2830	1160

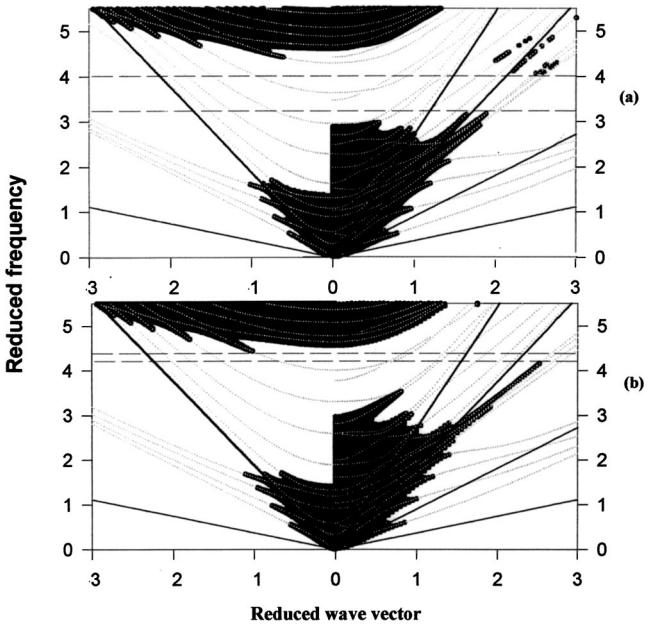

FIG. 3. Dispersion curves of the cladded finite superlattice embedded between two substrates. The shaded area correspond to the frequency domain in which the transmission power can exceed a threshold of 10^{-3}. The thickness of the clad layer is $d_{Si}=8D$, and the superlattice contains four bilayers of Al and W. The clad is in contact either with an Al layer (a) or with a W layer (b). The left and right panels, respectively, refer to shear horizontal and sagittal acoustics modes. The horizontal dashed lines delimit the edges of the omnidirectional acoustic band gap. The heavy and thin straight lines, respectively, show the transverse sound lines of the substrate (epoxy) and the clad (Si).

the superlattice, whatever the frequency. Thus, the wave will be partially transmitted through the superlattice, and only partially reflected back, depending upon the incidence angle (or equivalently, upon the wave vector $k_{\|}$).

Therefore the occurrence of an omnidirectional band gap introduces a limitation regarding the choice of the substrate material, namely, this material should have relatively high acoustic velocities as compared to the typical velocities of the materials constituting the superlattice. In order to remove this limitation or at least facilitate the existence of an omnidirectional reflection band, we, respectively, present in the next two sections the solutions mentioned above. The first one consists of cladding the superlattice (SL) with a layer of high acoustic velocities, which can act like a barrier for the propagation of phonons. The second solution consists of considering a combination of two different superlattices, provided their band structures do not overlap over the frequency range of the omnidirectional band gap.

A. Cladded superlattice structure

This section contains results of the transmission spectra, density of states, and dispersion curves for acoustic modes in a finite Al/W SL cladded on one side by a Si layer of thickness d_{Si}, and embedded between two substrates made of epoxy (Fig. 1).

Figure 3 gives an example of the dispersion curves for the above structure, together with the frequency domains in which the transmission power exceeds a threshold of 10^{-3} (shaded areas). In this example, the thickness of the Si layer is $d_{Si}=8D$, and the superlattice contains four bilayers of Al and W; the clad layer is in contact with either an Al layer [Fig. 3(a)] or a W layer [Fig. 3(b)] in the superlattice [see Fig. 1(b)]. The branches that fall outside the minibands of the superlattice are essentially associated either with the guided modes of the Si layer or with the interface modes localized at the Si-superlattice boundary (the latter are located below the sound lines of Si).

As compared to the superlattice minigap, the omnidirectional reflection band (delimited by the two horizontal dashed lines in Fig. 3) can be significantly reduced. In the case of Fig. 3(b) where the omnidirectional gap almost disappears, the main limitation is due to transmission through the modes belonging to a narrow miniband of the superlattice; this corresponds to a narrow range of the incidence angle in the substrate (around 14°). Therefore, with the geometrical parameters chosen in this example, the clad layer is not efficient to bring the transmission below the threshold of 10^{-3} in a broad frequency range, for all incidence angles and all polarizations. Actually, increasing the threshold to 10^{-2} does not significantly improve the omnidirectional gap in this case. In the example of Fig. 3(a) where an Al layer in the superlattice is in contact with the Si clad, the omnidirectional gap extends from $\Omega=3.176$ to $\Omega=4$. Here the upper edge of the gap is decreased as compared to the superlattice minigap, due to transmission around the frequencies $\Omega=4-4.5$ (upper right corner of the figure). From right to left, the transmission occurs through bulk modes of the superlattice belonging to a narrow miniband, through an interface mode at the boundary between the superlattice and the Si-clad layer, and through a guided mode of the Si layer. Although the transmittance through the latter modes exceeds the chosen threshold of 10^{-3}, still it remains very small (see Fig. 5 below).

One can notice that the presence of the clad layer has two opposite effects. It decreases the transmittance in some frequency domains (essentially below the sound line defined by the transverse velocity of sound in the clad), but also introduces new modes that can contribute themselves to transmission. The transmission by the latter modes is prevented by the superlattice when the corresponding branches fall inside the minigaps.

To give a better insight into the behaviors of the transmission coefficients, we present in Figs. 4 and 5, for two values of $k_{\|}D$, the transmitted intensities through the cladded superlattice. For the sake of comparison, we have also given the densities of states. The results are presented for different polarizations, namely, the incident wave can be shear horizontal, transverse in the sagittal plane, or longitudinal, and the DOS is given for either shear horizontal or sagittal modes. The thickness of the Si layer is again $d_{Si}=8D$, the superlattice is composed of $N=4$ bilayers of Al and W, and the clad layer is in contact with an Al layer.

At $k_{\|}D=0$ (Fig. 4), corresponding to a normal incidence, there is a decoupling between waves of transverse and longitudinal polarizations. One can observe that the presence of

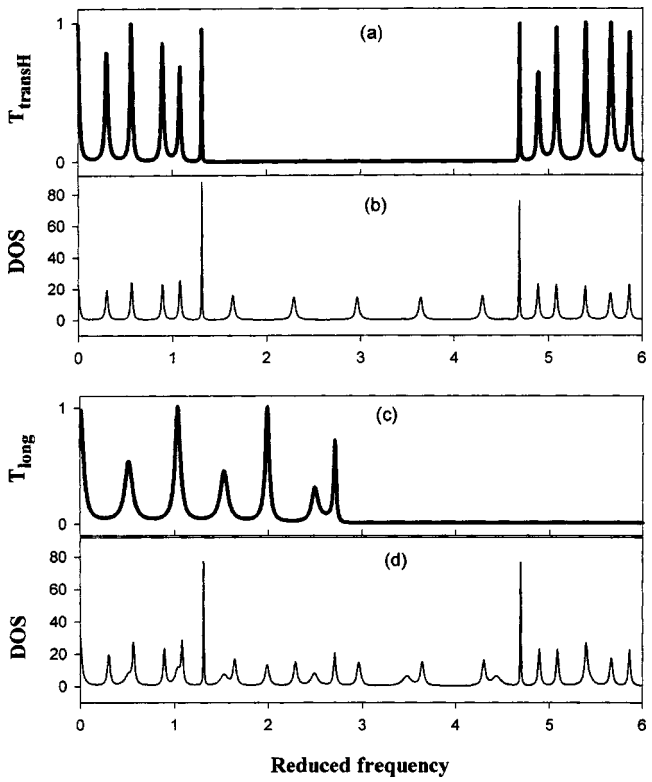

FIG. 4. Transmission coefficients and densities of states for the cladded superlattice structure of Fig. 3(a), at $k_{\|}D=0$. The panels (a) and (b) are plotted for acoustic waves of transverse polarization. Panels (c) and (d) refer to waves of longitudinal polarization.

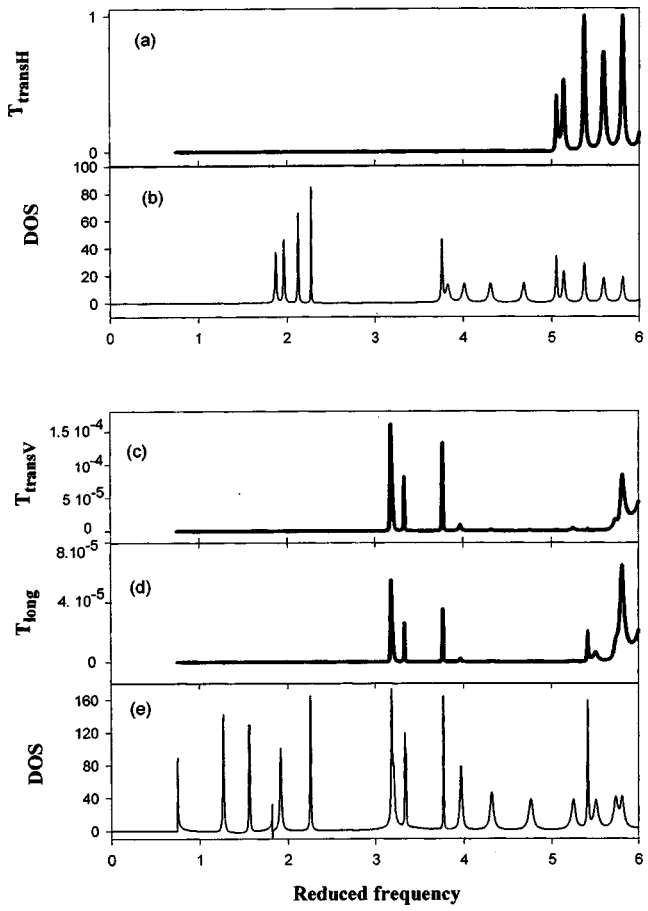

FIG. 5. Same as in Fig. 3 but for $k_{\|}D=2$. Panels (a), (c), and (d), respectively, give the transmission power for an incident wave of the following polarization: shear horizontal, transverse in the sagittal plane, and longitudinal in the sagittal plane (one can notice the small scales on the vertical axes of panels (c) and (d)). Panels (b) and (e) present the densities of states, respectively, associated with shear horizontal and sagittal waves.

the clad layer does not affect the band gap that is almost identical to the minigap of the superlattice ($2.95<\Omega<4.58$). The clad layer induces additional modes (see the peaks in the DOS), which are the guided modes of the Si layer, but these modes do not contribute to transmission when they fall inside the minigap of the superlattice (see, for instance, the peaks in DOS around the frequencies $\Omega=3-4$). At $k_{\|}D=2$ (Fig. 5), the presence of the clad layer of Si prevents the propagation of sound in the frequency range that lies below the transverse sound line of Si (Ω below 3.5). Hence, in this range of frequency, the clad layer plays the role of a barrier between phonons in the substrate and the superlattice, leading to a decrease in the transmitted intensity [please notice the very small scales in the vertical axes of Figs. 5(c) and 5(d)]. On the other hand, the modes induced by the Si layer, which fall in the superlattice minigap (around $\Omega=4.5$) contribute very weakly to the transmission process, as mentioned in connection with the discussion of Fig. 3(a).

To investigate the effect of superlattice termination on the existence of the omnidirectional gap, we have also considered, besides the examples of Fig. 3, two other cases; namely, the case of a superlattice containing $N+1=5$ layers of Al and $N=4$ layers of W (Al termination on both sides of the superlattice) and the case of a superlattice containing five layers of W and four layers of Al (W termination on both sides). These cases are less favorable than those presented in Fig. 3 and, more especially, the absolute acoustic gap disappears in the latter case.

We can now briefly discuss the existence and behavior of the omnidirectional reflection band as a function of the geometrical parameters involved in our structure, namely, the thickness d_{Si} of the Si layer and the number N of unit cells in the superlattice. The maximum tolerance for transmission is chosen to be either 10^{-3} or 10^{-2}. A detailed investigation of the transmission coefficients shows that the gap stabilizes for d_{Si} exceeding a thickness of $5.5D$ and N greater than 4. In Fig. 6, we present the variation of the gap as a function of d_{Si} for three values of N; namely, $N=5$, 8, and 10. In each case, the omnidirectional gap is sketched for both choices of the transmittance threshold.

First, let us notice that the limitation about the width of the absolute gap comes from the waves of sagittal polarization, since the gap in the shear horizontal polarization is relatively broad and already exists for values of d_{Si} and N of the order of $1.5D$ and 2, respectively. The sagittal gap shown in Fig. 6 widens with increasing the thickness of the Si layer, although some irregular behaviors can be noticed at the edges of the gap. It is even worth mentioning that for N below or equal to 4, the gap may close when going to in-

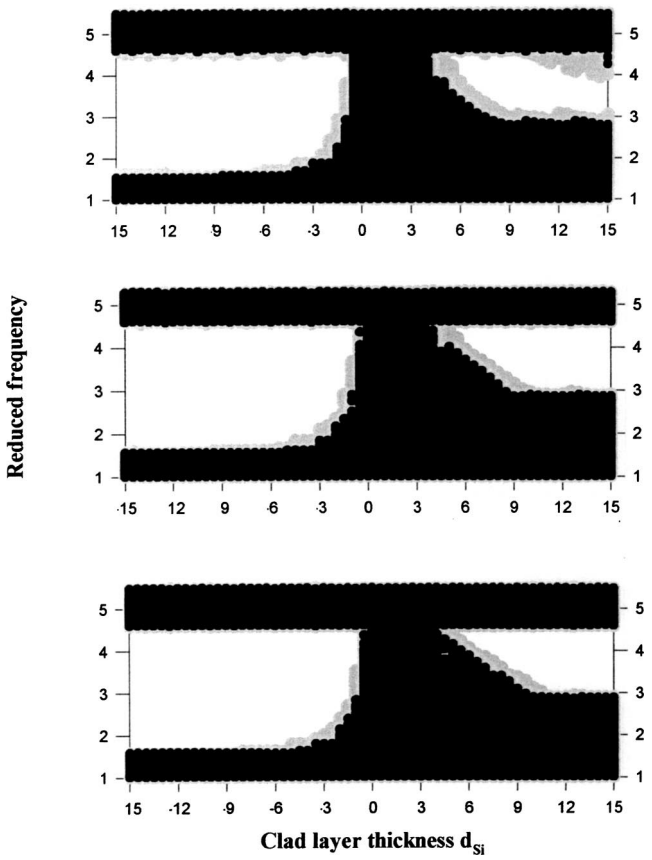

FIG. 6. Dependence of the omnidirectional gap with the thickness d_{Si} of the clad layer for different numbers of Al/W bilayers in the superlattice: (a) $N=5$, (b) $N=8$, and (c) $N=10$. The gray and dark areas, respectively, correspond to the frequency domains where the transmission exceeds 10^{-3} or 10^{-2}. The left and right panels, respectively, refer to shear horizontal and sagittal acoustic modes.

creasing value of d_{Si}; this means that the transmission through the guided modes of the clad layer are not efficiently prevented by the superlattice. From Fig. 6, one can conclude that the acoustic gap almost reaches its maximum value for $N=6$ and $d_{Si}=11D$. For the sake of completeness, we also present in Fig. 7 the variation of the gaps as a function of the number of unit cells in the superlattice, for $d_{Si}=8D$.

Finally, we have compared the behavior of the transmission coefficients when an additional Si layer is inserted at different places inside the superlattice. It turns out that the best solution is obtained when the Si layer is added as a clad, i.e., at the boundary of the superlattice. More precisely, with $N=4$ and $d_{Si}=8D$, there is no absolute gap when the Si layer is inserted inside the superlattice.

B. Coupled multilayer structures

In this section, we study the transmission of acoustic waves through a layered structure composed of two coupled superlattices [Fig. 1(d)] chosen in such a way that the superposition of their band structure displays an absolute band gap. This means, in some frequency range, the minibands of one superlattice overlap with the minigaps of the other, and vice versa.

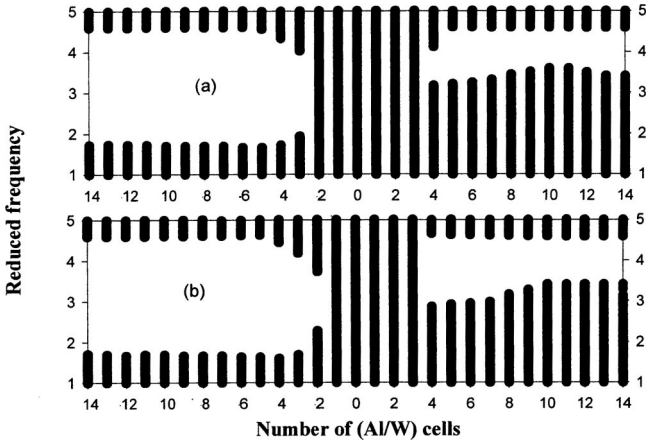

FIG. 7. Dependence of the omnidirectional gap with the number N of unit cells in the Al/W superlattice. The Si clad is in contact with an Al layer and has a thickness of $d_{Si}=8D$. The transmission threshold is fixed to 10^{-3} (a) and 10^{-2} (b).

We have investigated several possibilities of elastic and geometrical parameters for the coupled superlattice structure. Among a few possibilities that give rise to the occurrence of an omnidirectional band gap, one interesting solution consists of combining the Al/W superlattice with a Fe/epoxy superlattice of the same period D but with $d_1'=0.8D$ and $d_2'=0.2D$. The superposition of the band structures for these superlattices is presented in Fig. 8 and clearly displays a broad absolute acoustic gap in the frequency range $2.54<\Omega<5.29$ (delimited by the dashed horizontal lines). One can expect that in this frequency domain, any wave generated in any substrate will be totally reflected. In practice, the coupled superlattice structure is of finite width, and one can only impose a maximum tolerance on the transmission coefficients.

In the following, we assume that the substrates are made of a low-velocity material such as epoxy. Figure 9 displays the dispersion curves of the coupled superlattice structure

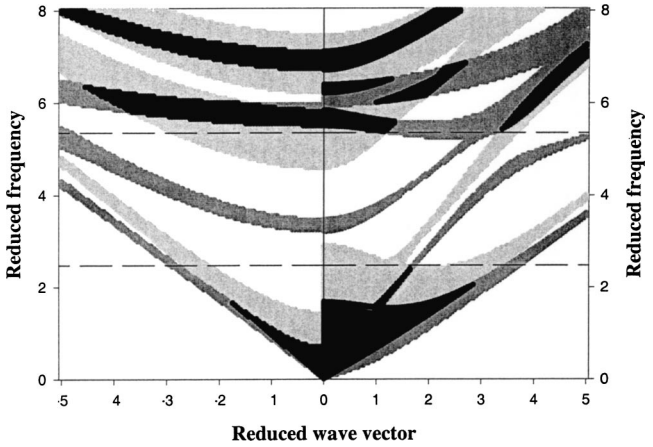

FIG. 8. Projected band structures of two different superlattices, namely, Al/W (bright gray) and Fe/epoxy (dark gray). The overlap between both band structures is presented as black areas. The right and left panels represent the sagittal and the transverse band structures, respectively.

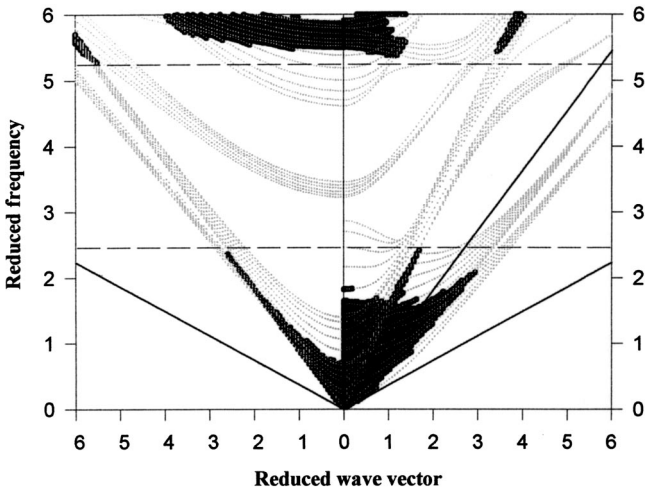

FIG. 9. Dispersion curves of two finite superlattices combined in tandem and embedded between two substrates. The shaded area corresponds to the frequency domain in which the transmission power can exceed a threshold of 10^{-3}. The Al/W superlattice contains $N+1=9$ layers of Al and $N=8$ layers of W. The epoxy/Fe superlattice contains $N'+1=6$ layers of epoxy and $N'=5$ layers of Fe.

together with the frequency domains in which the power transmission does not exceed a threshold of 10^{-3}. The finite system is composed of an Al/W superlattice containing nine layers of Al and eight layers of W, and an epoxy/Fe superlattice with six layers of epoxy and five layers of Fe. The omnidirectional reflection band extends from 2.48 to 5.35, and practically coincides with the complete acoustic gap of Fig. 8. Let us notice that there is an interface mode at the boundary between epoxy and the Al/W superlattice (see the branch in the upper right corner of Fig. 9, around $k_{\|}D=4-5$ and Ω around 5.5–6); however, this mode does not contribute noticeably to transmission. It is worth mentioning that the choice of the materials that are the terminal layers in each superlattice is important for the omnidirectional gap to exist and to have a relatively large bandwidth. Another illustration for the occurrence of the omnidirectional gap is presented in Fig. 10 where we give, at $k_{\|}D=2.5$, the transmission coefficients for different polarizations of the incident wave, together with the density of states of transverse and sagittal modes. It can be seen that the modes of each superlattice that fall inside a gap of the other superlattice contribute only a negligible amount to the transmission power.

Finally, in Fig. 11, we sketch the effect of the numbers N and N' of unit cells in each superlattice on the transmission power. The absolute gap is presented by assuming that the transmission remains below the threshold of 10^{-3}. The absolute gap starts to open for N and N' respectively higher than 4 and 7, respectively [Fig. 11(a)]. However, it is necessary to take values such as $N=8$ and $N'=6$ to obtain a relatively broad reflection band. Going to higher values of N and N' stabilizes the gap width without a noticeable modification.

IV. SUMMARY

In this paper, we have developed the idea that 1D lamellar structures can exhibit an omnidirectional reflection band,

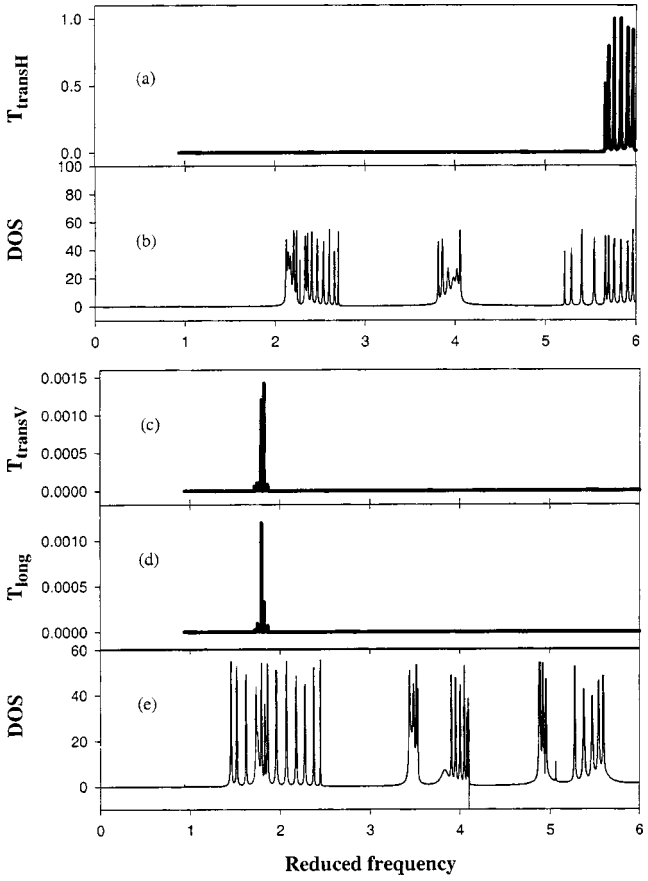

FIG. 10. Transmission coefficients and density of states for the coupled (Al/W) and (epoxy/Fe) superlattices, at $k_{\|}D=2.5$. The other descriptions are the same as in Fig. 5.

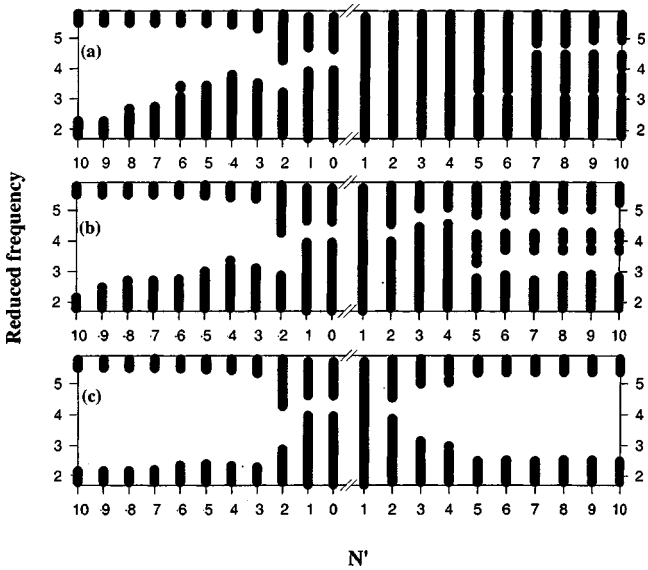

FIG. 11. Dependence of the omnidirectional gap with the number N' of unit cells in the epoxy/Fe superlattice, for different numbers of unit cells in the Al/W superlattice: (a) $N=3$, (b) $N=4$, and (c) $N=8$. The transmission threshold is fixed to 10^{-3}.

anologous to the case of 2D and 3D phononic crystals. This property can be fulfilled with a superlattice when the velocities of sound in the substrate are higher than the characteristic velocities of the superlattice constituents. In the more general case when the substrate is made of a soft material, we have proposed two solutions to realize the omnidirectional mirror, namely, the cladding of a superlattice with a hard material that acts like a barrier for the propagation of phonons, or a combination in tandem of two different superlattices in such a way that their band structures do not overlap over a given frequency range. The latter solution gives rise to a relatively broad band gap, provided an appropriate choice of the material and geometrical properties is made. With the former solution, the contribution of the guided modes induced by the clad layer to power transmission should be more carefully taken into account. The thickness of the clad layer, the number of unit cells in the superlattices, as well as the nature of the terminal layers in the superlattices involved in the structure are also important parameters for determining the maximum tolerance for power transmission. The results presented in this paper, namely, transmission coefficients, densities of states, and dispersion curves, are based on analytical calculations of the Green's functions for acoustic waves of shear horizontal and sagittal polarizations in composite lamellar structures.

[1] M. S. Kushwaha, P. Halevi, L. Dobrzynski, and B. Djafari-Rouhani, Phys. Rev. Lett. **71**, 2022 (1993).

[2] M. Sigalas and E. N. Economou, Solid State Commun. **86**, 141 (1993).

[3] M. S. Kushwaha, B. Djafari-Rouhani, and L. Dobrzynski, Phys. Lett. A **248**, 252 (1998).

[4] F. R. Montero de Espinoza, E. Jimenez, and M. Torres, Phys. Rev. Lett. **80**, 1208 (1998).

[5] J. O. Vasseur, P. A. Deymier, G. Frantziskonis, G. Hong, B. Djafari-Rouhani, and L. Dobrzynski, J. Phys.: Condens. Matter **10**, 6051 (1998).

[6] D. Caballero, J. Sanchez-Dehesa, C. Rubio, R. Martinez-Sala, J. V. Sanchez-Perez, F. Meseguer, and J. Llinares, Phys. Rev. E **60**, R6316 (1999).

[7] For a review, see M. S. Kushwaha, Int. J. Mod. Phys. B **10**, 977 (1998).

[8] See, for example, *Photonic Crystals*, edited by J. D. Joannopoulos, R. D. Meade, and J. N. Winn (Princeton University Press, Princeton, NJ, 1995); *Photonic Crystals and Light Localization in the 21st Century*, Vol. 563 of *NATO Advanced Study Institute, Series C: Mathematical and Physical Sciences*, edited by C. M. Soukoulis (Kluwer, Dordrecht, 2001).

[9] V. Narayanamurti, Science **213**, 717 (1981).

[10] K. Sagami, H. Gen, M. Morimoto, and D. Takahashi, Acoustica **82**, 45 (1996).

[11] S. D. Cheng, Y. Y. Zhu, Y. L. Lu, and N. B. Ming, Appl. Phys. Lett. **66**, 291 (1995).

[12] J. P. Dowling, Science **282**, 1841 (1998).

[13] Y. Fink, J. N. Winn, S. Fan, C. Chen, J. Michel, J. D. Joannopoulos, and E. L. Thomas, Science **282**, 1679 (1998).

[14] D. N. Chigrin, A. V. Lavrinenko, D. A. Yarotsky, and S. V. Gaponenko, Appl. Phys. A: Mater. Sci. Process. **A68**, 25 (1999).

[15] D. Bria, B. Djafari-Rouhani, E. H. El Boudouti, A. Mir, A. Akjouj, and A. Nougaoui, J. Appl. Phys. **91**, 2569 (2002).

[16] A. Bousfia, E. H. El Boudouti, B. Djafari-Rouhani, D. Bria, A. Nougaoui, and V. R. Velasco, Surf. Sci. **482**, 1175 (2001).

[17] D. Bria, B. Djafari-Rouhani, A. Bousfia, E. H. El Boudouti, and A. Nougaoui, Europhys. Lett. **55**, 841 (2001).

[18] L. Dobrzynski, Surf. Sci. Rep. **11**, 139 (1990), and references therein.

[19] L. Dobrzynski and H. Puszkaski, J. Phys.: Condens. Matter **1**, 1239 (1989).

[20] E. H. El Boudouti, Thèse d'état, Université d'Oujda, Maroc, 1998 (unpublished); D. Bria, Thèse d'état, Université d'Oujda, Maroc, 2000, (unpublished); D. Bria, E. H. El Boudouti, A. Nougaoui, B. Djafari-Rouhani, and V. R. Velasco, Phys. Rev. B **60**, 2505 (1999).

[21] B. Djafari-Rouhani and L. Dobrzynski, J. Phys.: Condens. Matter **5**, 8177 (1993).